International Journal of Robotics and Control Systems
Vol. 5, No. 1, 2025, pp. 333-347
ISSN 2775-2658
http://pubs2.ascee.org/index.php/ijrcs

Optimized Vector Control Using Swarm Bipolar Algorithm for Five-Level PWM Inverter-Fed Three-Phase Induction Motor

Farazdaq R. Yaseen [a,1], Huthaifa Al-Khazraji [a,2,*]

[a] Control and System Engineering Department, University of Technology-Iraq, Baghdad 10066, Iraq
[1] 60002@uotechnology.edu.iq; [2] 60141@uotechnology.edu.iq
* Corresponding Author

ARTICLE INFO

Article history
Received November 12, 2024
Revised December 20, 2024
Accepted December 29, 2024

Keywords
Three Phase Induction Motor;
Vector Control;
Control Systems;
Five-Level SPWM;
Five-Level SVPWM;
Swarm Bipolar Algorithm;
Optimization;
Threshold Harmonic Distortion

ABSTRACT

Induction motors (IMs) are commonly used in various applications such as robotics and automotive industries. This paper proposes an optimization of two proportional-integral (PI) controllers for a multi-level pulse width modulation (PWM) voltage-fed inverter linked to a three-phase IM. The paper aims to enhance inverter output quality, minimize harmonic distortion, and ensure robust, stable performance. The swarm bipolar algorithm (SBA) is introduced to elaborate the searching of the best settings of the PI controllers to achieve the desired response. Harmonics lead to increased system losses by creating negative torque components. To address this problem, two modulation algorithms are proposed to generate three-phase voltage with minimum harmonics including space vector PWM (SVPWM) inverter and sinusoidal PWM (SPWM). Simulation results based on MATLAB/Simulink environment for various operation conditions such as sudden loads change and speed changes reveal that the proposed controller enhances the system's performance. Moreover, the five-level SVPWM inverter has a minimum threshold harmonic distortion (THD) compared to the five-level SPWM inverter where the THD is decreased from 40.24% for SPWM method to 13.67% for the SVPWM method.

1. Introduction

Most engineering drive applications, such as robotics, use induction motors (IMs) with complex and unpredictable behaviors [1]. Feedback control algorithms have consistently improved system performance [2]-[9]. The development of high-performance control techniques for IMs has advanced quickly. IM control algorithms fall into two main categories: scalar control, which includes open-loop voltage/frequency control, slip frequency methods, and vector control. Scalar control methods are simple, cost-effective, and easy to design. In contrast, vector controllers are advanced devices that manage both the strength and direction of voltage or current. However, they are often costly [10]. IMs must operate across a wide range of speeds. Controlling their speed is difficult because the rotor and stator are directly connected. Vector control offers a solution to this challenge. It allows us to control an AC motor similarly to a DC motor, giving us similar performance. Generally, controlling an IM involves two loops: one loop to manipulate the current, and the other loop focuses on keeping track of the speed [11]. To enhance motor performance, we must eliminate harmonics in the inverter's output voltage and frequency [12]. Harmonics are

multiples of the main frequency in electrical systems, generated by nonlinear loads, switching devices, and flux effects. They can lead to increased system losses by creating negative torque components.

Inverters convert direct current (DC) to alternating current (AC) and are studied for performance based on voltage and frequency. Choosing the right number of levels, modulation methods, and inverter types is crucial for enhancing performance. Key goals include reducing Total Harmonic Distortion (THD), broadening the linear modulation range, minimizing switching losses, and simplifying installation. Sinusoidal Pulse Width Modulation (SPWM) and Space Vector PWM (SVPWM) are common modulation techniques [12]. In SPWMs, the inverter is viewed as three distinct push-pull driver stages, with each phase waveform produced independently. In contrast, SVPWM considers the inverter a single entity operating in eight states. SVPWM is preferred mainly because of its straightforward implementation, superior harmonics performance, enhanced DC voltage utilization ratio, lower switching losses, and ease of capacitor voltage balancing [13]. Researchers are examining inverter performance at different levels. There are two main types: two-level inverters and multilevel inverters, with the latter capable of operating at various voltage levels [14]. More levels in the SVPWM inverter lead to more switching states and triangles, complicating the calculation of on-time periods for switching [13]. A three-level inverter features 27 switching states and has 24 triangles represented in its space vector diagram, whereas a five-level inverter displays 125 switching states and 96 triangles. Different inverters consist of diode-clamped, H-bridge, and flying capacitor configurations [15]. The diode-clamped inverter, known as the Neutral point-clamped (NPC), is a preferred multilevel inverter design.

This paper explores the use of two optimized Proportional-Integral (PI) controllers for an IM under varying load and speed conditions using MATLAB/SIMULINK. The main aim is to reduce THD through modulation algorithms. It also evaluates the performance of a five-level Sinusoidal Pulse Width Modulated (5LSPWM) inverter and a five-level Space Vector Pulse Width Modulated (5LSVPWM) inverter, both with a closed-loop vector control system for the IM.

2. Vector Control

The stator flux vector ($\bar{\varphi}_s$) of the IM can be obtained from measurements of current ($\bar{\imath}_s$) and voltage ($\bar{V}_s$) according to stator voltage equation in the stationary reference frame as given by [16]:

$$\bar{\varphi}_s = \int (\bar{V}_s - \bar{\imath}_s R_s) dt \tag{1}$$

Where R_s is the stator winding resistance. It is necessary to transform the measured stator currents form stationary abc system to αβo system by using Clarke transform as follows:

$$\begin{bmatrix} I_\alpha \\ I_\beta \\ I_o \end{bmatrix} = M \begin{bmatrix} I_a \\ I_b \\ I_c \end{bmatrix} \tag{2}$$

Where M is the transformation matrix and it's given by:

$$M = \frac{1}{3}\begin{bmatrix} 2 & -1 & -1 \\ 0 & \sqrt{3} & -\sqrt{3} \\ 1 & 1 & 1 \end{bmatrix}$$

In the same way, the vector of the stator voltage in abc system is transformed to αβo system as follows:

$$\begin{bmatrix} V_\alpha \\ V_\beta \\ V_o \end{bmatrix} = M \begin{bmatrix} V_a \\ V_b \\ V_c \end{bmatrix} \tag{3}$$

The developed torque (T_e) is estimated by

$$T_e = \frac{3}{2}\frac{P}{2}(\varphi_{s\alpha} i_\beta - \varphi_{s\beta} i_\alpha) \quad (4)$$

Where

$$\varphi_{s\alpha} = \int (\bar{V}_\alpha - \bar{\imath}_\alpha R_s) dt \quad (5)$$

$$\varphi_{s\beta} = \int (\bar{V}_\beta - \bar{\imath}_\beta R_s) dt \quad (6)$$

And

$$|\varphi_s| = \sqrt{\varphi_{s\alpha}^2 + \varphi_{s\beta}^2} \quad (7)$$

The magnitude of the reference vector V_r is calculated as

$$V_r = \sqrt{V_\alpha^2 + V_\beta^2} \quad (8)$$

While its orientation θ is given by [17]:

$$\theta = \tan^{-1}\frac{V_\beta}{V_\alpha} \quad (9)$$

The modulation index m is given by [18]:

$$m = \frac{\sqrt{3}\, V_r}{V_{dc}} \quad (10)$$

3. Optimized PI Controller

This section outlines the design of a simple and effective proportional-integral (PI) controller for an IM system. The PI controller is a common method in control systems, using two inputs: the error and the accumulated process to generate a control signal for performance regulation [19]-[21]. The PI controller control law is defined as follows:

$$u(t) = K_p e(t) + K_i \int_0^t e(t) dt \quad (11)$$

Where

$u(t)$: Control Law

$e(t)$: Error

K_p : Proportional Gain

K_i : Integral Gain

The PI controller has a simple structure, but proper tuning is essential for performance. Instead of trial and error, we can optimize the tuning of its design variables [22]-[25]. Swarm optimization finds optimal values for the design variables of various industrial and control engineering problems

[26]-[32]. In this scenario, the swarm bipolar algorithm (SBA) determines the optimal values for the PI controller's design variables.

The SBA is a swarm optimization method presented by Kusuma and Dinimaharawati in 2024 [33]. It divides individuals into two equal sub-groups and starts by spreading them across the search space [34]. The algorithm employs four strategies to find optimal solutions:

1. Move towards the best member of the entire group.
2. Move towards the best member of each sub-group.
3. Move towards the midpoint of the best members from both sub-groups.
4. Move randomly towards selected members of the other sub-group.

The effectiveness of the SBA relies on its procedural implementation, mathematically formulated between Eq. (12) and Eq. (21), starting with the initial solution in Eq. (12) and updating the best members in Eq. (13) remembers, respectively [35].

$$p_i = p_l + r_1(p_u - p_l) \tag{12}$$

$$p_b = \begin{Bmatrix} p_i, f(p_i) < f(p_b) \\ p_b, \text{else} \end{Bmatrix} \tag{13}$$

$$p_{sb1} = \begin{Bmatrix} p_i, f(p_i) < f(p_{sb1}) \wedge 1 \le i \le \frac{N_{pop}}{2} \\ p_{sb1}, \text{else} \end{Bmatrix} \tag{14}$$

$$p_{sb2} = \begin{Bmatrix} p_i, f(p_i) < f(p_{sb2}) \wedge \frac{N_{pop}}{2} < i < N_{pop} \\ p_{sb2}, \text{else} \end{Bmatrix} \tag{15}$$

Where

N_{pop} : population size

i : index for swarm member

p_i : swarm member

p_{PB} : finest swarm member

p_{PSB} : finest sub-swarm member

p_l : lower boundary

p_u : upper boundary

$f(.)$: cost function

r_1 : random number [0,1]

Equations (16) to (20) describe four search strategies to find the best solution:

1. Equation (16) directs each swarm member toward the best overall member.
2. Equation (17) focuses on finding the best member within a smaller group.
3. Equation (18) seeks the midpoint between the two best members of smaller groups.
4. Equation (19) involves searching for a randomly chosen member from another smaller group [36].

$$p_i(t+1) = r_1\left(p_b - r_2 p_i(t)\right) + p_i(t) \tag{16}$$

$$p_i(t+1) = \begin{cases} r_1(p_{sb1} - r_2 p_i(t)) + p_i(t), & 1 \le i \le \frac{N_{pop}}{2} \\ p_i(t) + r_1(p_{sb2} - r_2 p_i(t)), & \frac{N_{pop}}{2} \le i \le N_{pop} \end{cases} \quad (17)$$

$$p_i(t+1) = r_1\left(\frac{s_{sb1}+s_{sb2}}{2} - r_2 p_i(t)\right) + p_i(t) \quad (18)$$

$$p_i(t+1) = p_i(t) + r_1(p_k - r_2 p_i(t)) \quad (19)$$

Where

i : index for iteration

p_k : swarm member randomly chosen

r_1 : random number [1,2]

The Integral Time of Absolute Errors (ITAE) as given in Eq. (20) [2] is employed as a cost function to optimize the two PI controllers to ensure robust and stable performance of the IM.

$$ITAE = \int_{t=0}^{t=t_{sim}} t|e(t)|dt \quad (20)$$

Where t_{sim} is the simulation time.

4. Multi-Level PWM Inverter

Inverters are power electronics device that are utilized to convert the DC power to AC power at a level of the desired output voltage and frequency level. Multilevel inverters (MLIs) supply energy to IMs and offer advantages over traditional two-level inverters, such as reduced harmonic distortion, lower voltage variations (dv/dt), improved output performance, and lower switching frequencies [37]-[39]. More levels improve the output voltage waveform, producing a sinusoidal voltage without costly filters or bulky transformers [14]. The performance of multilevel inverters depends on the PWM algorithm, with Sinusoidal PWM (SPWM) and Space Vector PWM (SVPWM) being two commonly used options [40]-[41]. Various PWM designs for Multilevel Inverters (MLI) include H-bridge cascaded, flying capacitors, and diode-clamped inverters [42]. Choudhury et al. (2018) [43] presented a comparative study to examine the impact of the cascaded H-bridge and diode clamped MLIs on the THD. Diode clamped inverters use diodes to reduce the voltage stress of power devices whereas H-bridge cascaded inverters use the strings of single phase full bridge inverters which are linked in series to construct the phase legs of multilevel with separate dc sources. Based on Fast Fourier Transform (FFT), it was found out that the corresponding THD value was relatively low for diode-clamped as compared to H-bridge cascaded. Based on this result, the diode-clamped inverters with two PWM MLIs are described in the following subsection, including the 5LSPWM inverter and the 5LSVPWM inverter.

4.1. Five-Level SPWM Inverter

In the 5LSPWM inverter, each one of the three sinusoidal reference signals are compared with four triangle carrier signals [44] as shown in Fig. 1. The four comparators generate trigger pulses for eight IGBT transistors as shown in Fig. 2 and the response's voltage output line is shown in Fig. 3.

4.2. Five-Level SVPWM Inverter

The space vector diagram of the five-level inverter is shown in Fig. 4 [45]-[47]. It comprises six diagrams representing three-level inverters. These three-level diagrams are then broken down into six diagrams for two-level inverters. Choose one hexagon from the options to find the right

reference voltage [48]. Once the hexagon is chosen, the reference voltage vector is adjusted to align with that hexagon's center. Then, the rotate of the angle θ which is based on the number of the sector number is determined as shown in Table 1. This will allow converting the vector of voltage into an equivalent Sector 1 vector. The normalized value of the space vector (v') can be computed using the (α, β, o) coordinate system as follows:

$$v'_\alpha = v'\cos\theta' - v'\sin\theta'/\sqrt{3} \tag{21}$$

$$v'_\beta = v'\sin\theta' 2/\sqrt{3} \tag{22}$$

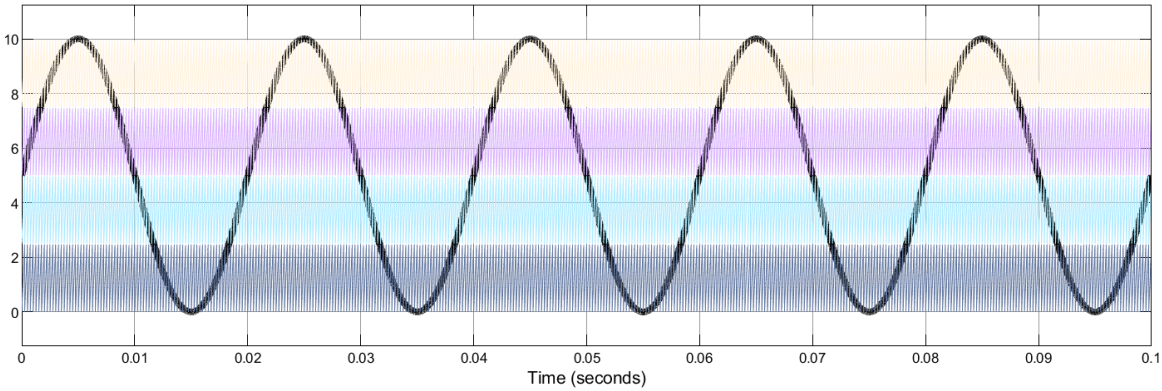

Fig. 1. Sinusoidal reference signals

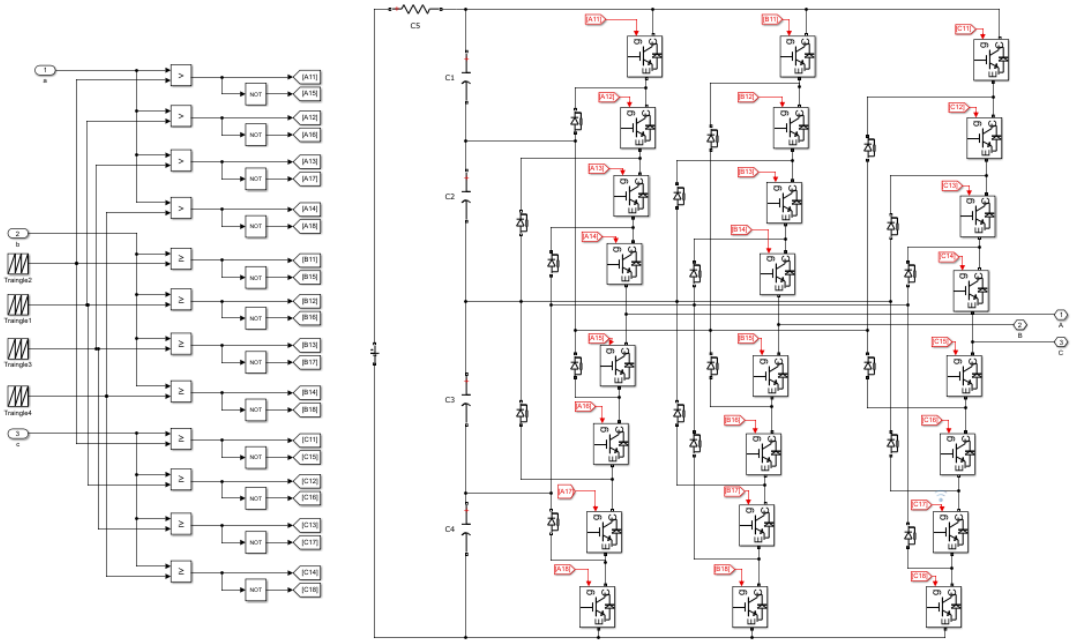

(a) Triggering circuit (b) Switching circuit

Fig. 2. Five-level SPWM invertor

The space vector v' is transformed into the matrix as given in Eq. (23) [49]:

$$\begin{bmatrix} V_D \\ V_E \\ V_F \\ V_G \end{bmatrix} = \begin{bmatrix} \text{floor}\,(v'_\alpha) & \text{floor}\,(v'_\beta) \\ \text{ceil}\,(v'_\alpha) & \text{floor}\,(v'_\beta) \\ \text{floor}\,(v'_\alpha) & \text{ceil}\,(v'_\beta) \\ \text{ceil}\,(v'_\alpha) & \text{ceil}\,(v'_\beta) \end{bmatrix} \tag{23}$$

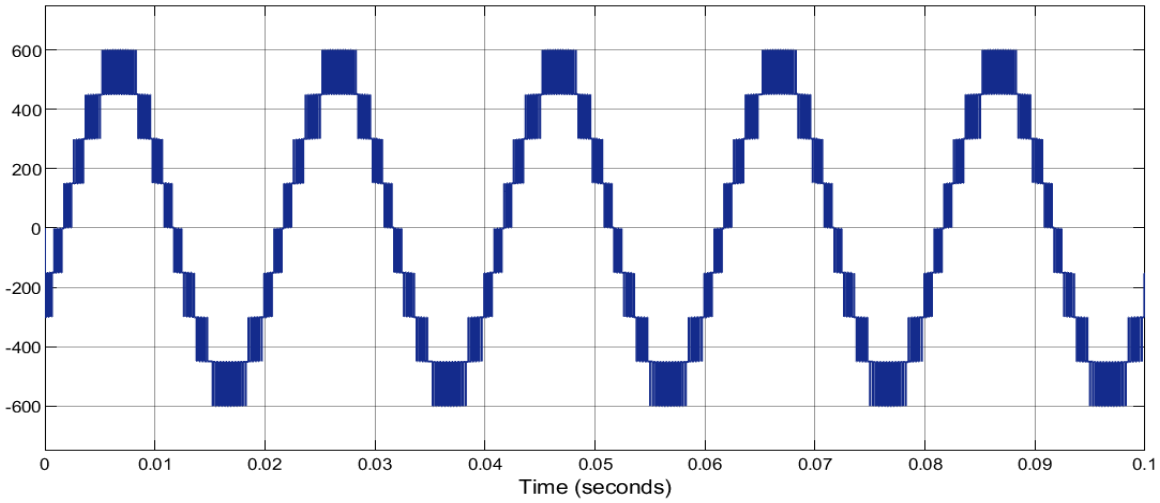

Fig. 3. Line voltage of five-level SPWM inverter

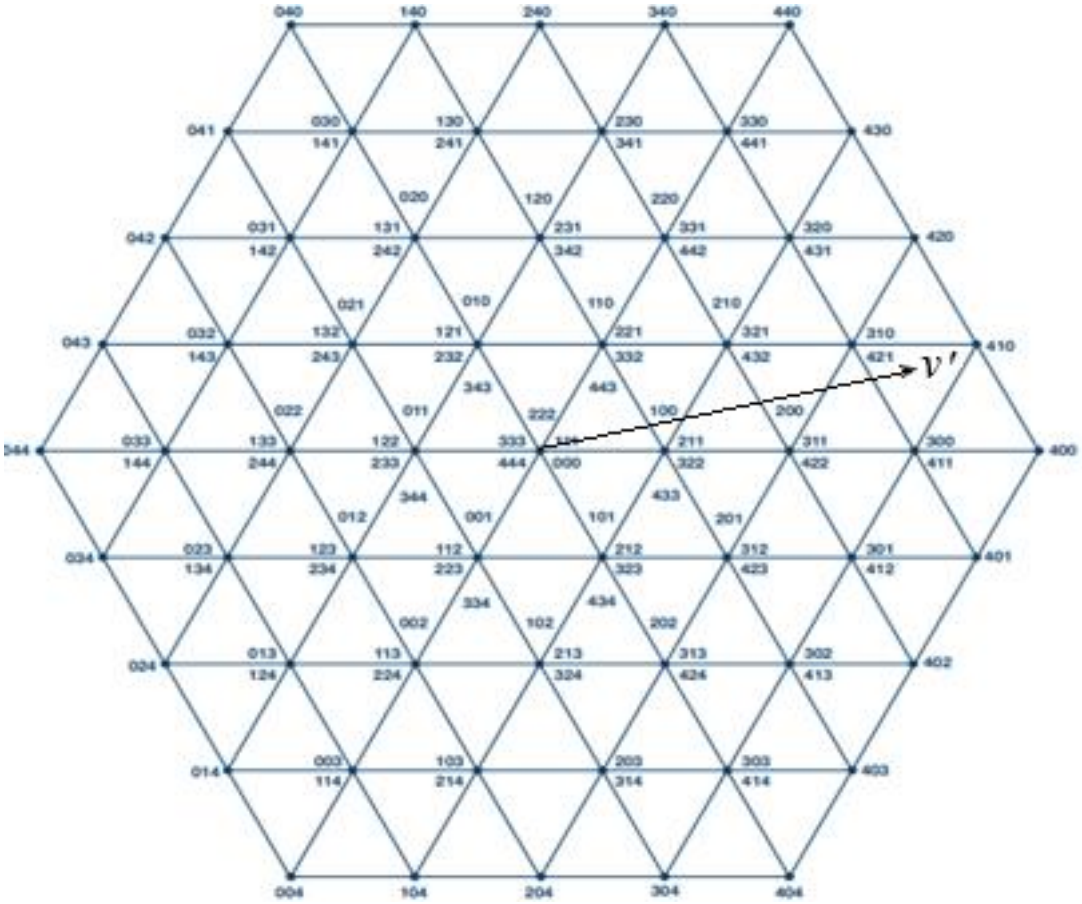

Fig. 4. Five-level SVPWM diagram

In order to convert the vectors to the original sector, the vectors in Eq. (23) are multiplied as shown in Eq. (24).

$$\begin{bmatrix} V'_D \\ V'_E \\ V'_F \\ V'_G \end{bmatrix} = \begin{bmatrix} V_D \\ V_E \\ V_F \\ V_G \end{bmatrix} \begin{bmatrix} u_\alpha \\ u_\beta \end{bmatrix} \tag{24}$$

Table 1. Sector selection

Sector	Angle (θ)	New (θ')	Vector u_a	Vector u_b
1	$(0, \frac{\pi}{3})$	$\theta' = \theta$	[1 0 0]	[1 1 0]
2	$(\frac{\pi}{3}, \frac{2\pi}{3})$	$\theta' = -\theta + \frac{2\pi}{3}$	[1 1 0]	[1 1 0]
3	$(\frac{2\pi}{3}, \pi)$	$\theta' = \theta - \frac{2\pi}{3}$	[0 1 0]	[0 1 1]
4	$(\pi, \frac{4\pi}{3})$	$\theta' = -\theta - \frac{2\pi}{3}$	[0 0 1]	[0 1 1]
5	$(\frac{4\pi}{3}, \frac{5\pi}{3})$	$\theta' = \theta + \frac{2\pi}{3}$	[0 0 1]	[1 0 1]
6	$(\frac{5\pi}{3}, 2\pi)$	$\theta' = -\theta$	[1 0 0]	[1 0 1]

The triggering circuit provides 24 pulses to 24 IGBT switch as shown in Fig. 5.

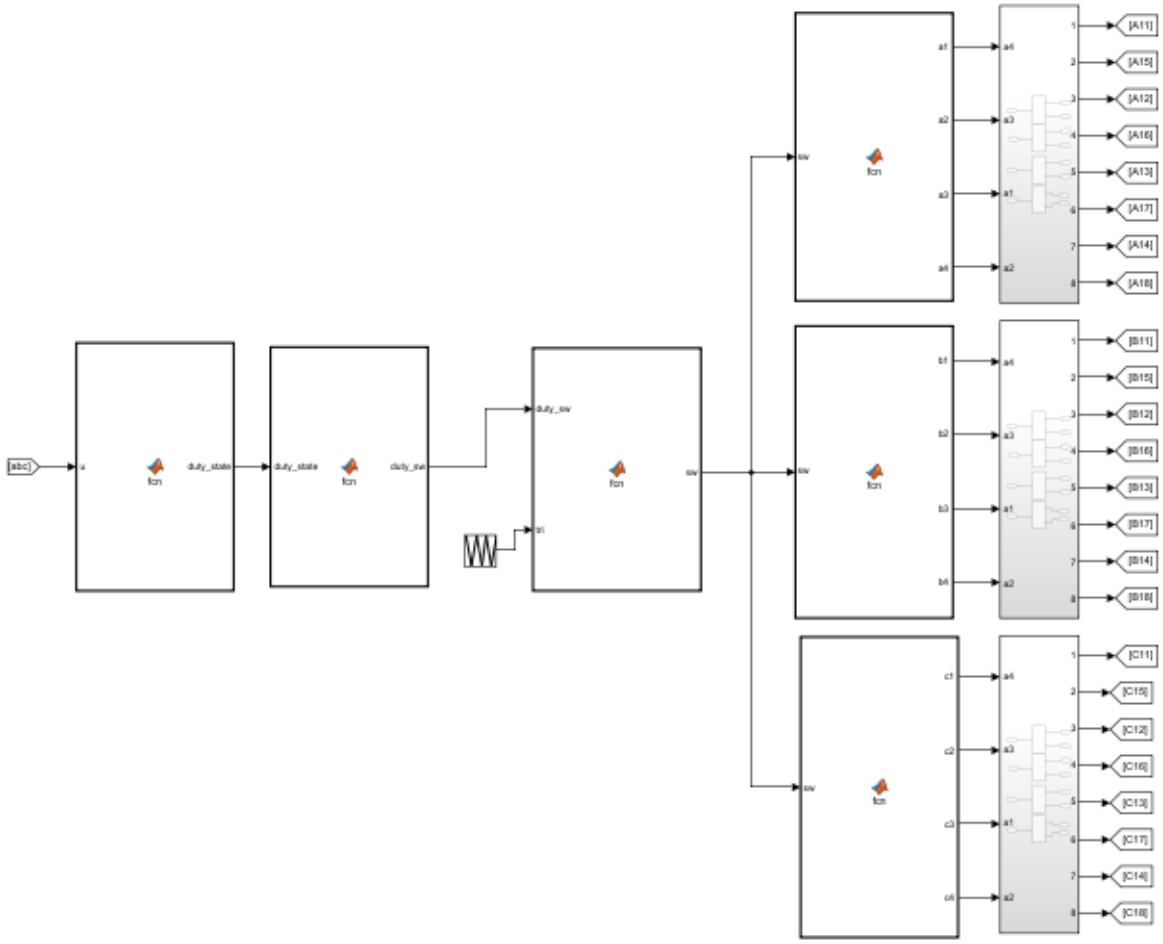

Fig. 5. Five-level SVPWM triggering circuit

5. Results and Discussion

In this section, the two multilevel inverter strategies including five levels SVPWM inverter and the five levels SPWM inverter are investigated to provide three phase voltage to the IM. The Simulink model of the VC strategy of IM is shown in Fig. 6. The model parameters are summarized in Table 2, [50].

Two PI controllers were used to control the IM. The first PI controller is used as a speed controller by estimating the required torque from the error between the desired speed and the actual

speed. The second PI controller is used to estimate the required orientation of the reference space vector. The two controllers' parameters are optimized based on the SBA with a cost function (ITAE=0.4365) and summarized in Table 3. The generated line voltage with its THD for the three multilevel inverter strategies is shown in Fig. 7. The harmonic content that is generated in the voltage waveforms produced by the two MLIs is reported in Table 4. The speed response, stator currents, and the rotor angle are shown in Fig. 8, Fig. 9, Fig. 10 respectively.

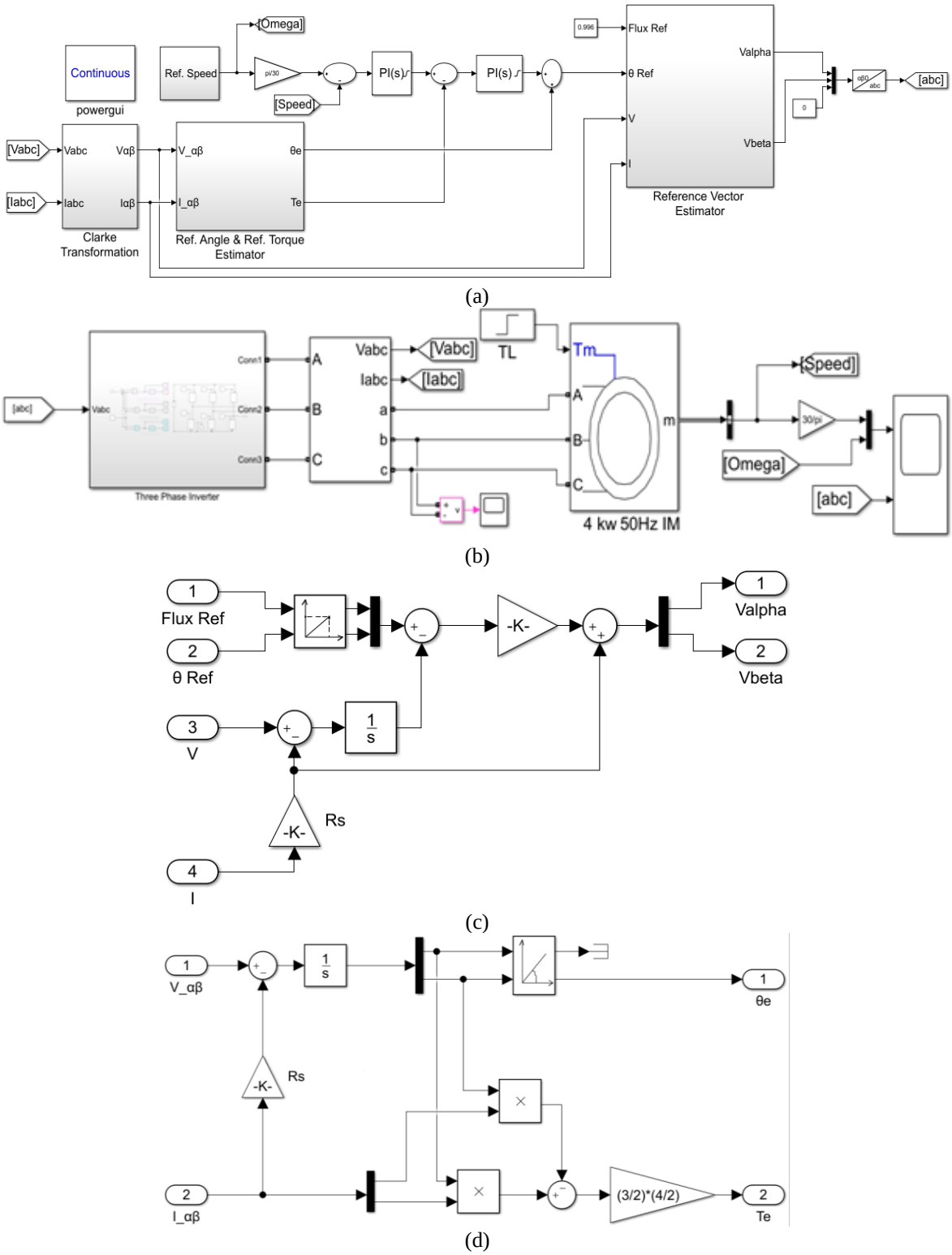

Fig. 6. Vector control scheme of three phases IM

Table 2. Three Phase Induction Motor 5.4 Hp (4kW) 400 V, 50Hz

Parameters	Symbols	Values
Mutual inductance	L_m	0.1722 H
Stator resistance	R_s	1.405 Ω
Rotor resistance	R'_r	1.395 Ω
Rotor inductance	L'_r	0.005839 H
Stator inductance	L_s	0.005839 H
Friction factor	F	0.002985 N.m.sec
Motor inertia	J	0.0131 kg.m2
No. of poles	P	4

Table 3. Gains of PI controllers

Gain	Torque Controller	Vector Orientation Controller
k_p	0.5	0.02
k_i	5	2

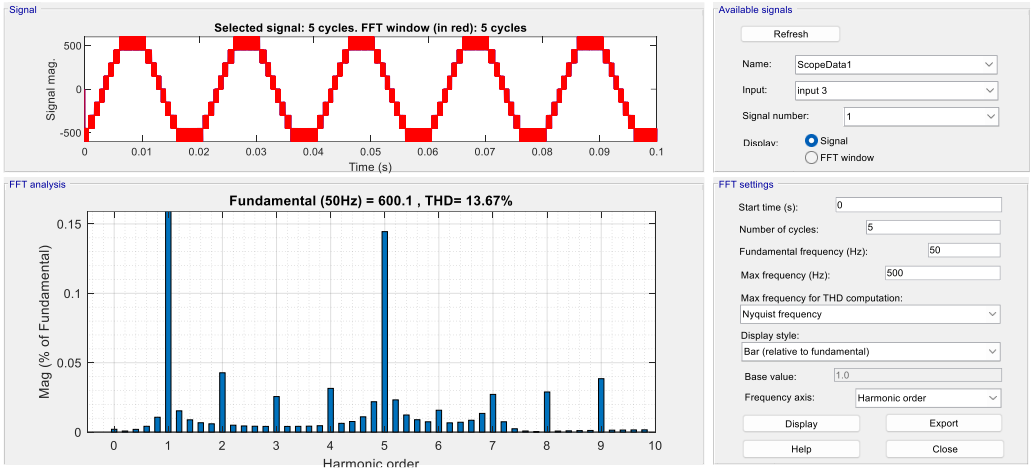

(a)

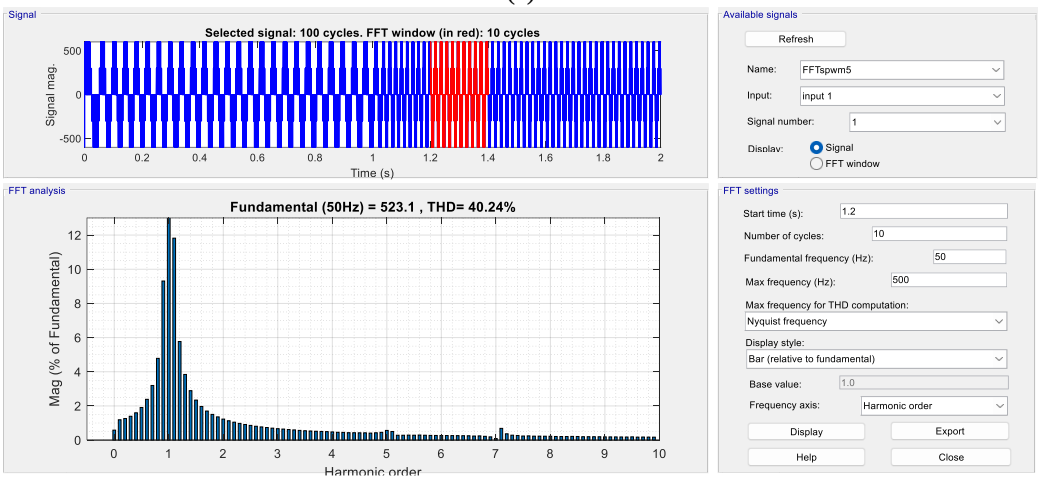

(b)

Fig. 7. (a) THD of voltage's output line of the five levels SVPWM inverter, (b) THD of voltage's output line of the five levels SPWM inverter

Table 4. Comparison among harmonic content in various multilevel inverter

Multilevel Inverter	%THD
Five levels SVPWM	13.67
Five levels SPWM	40.24

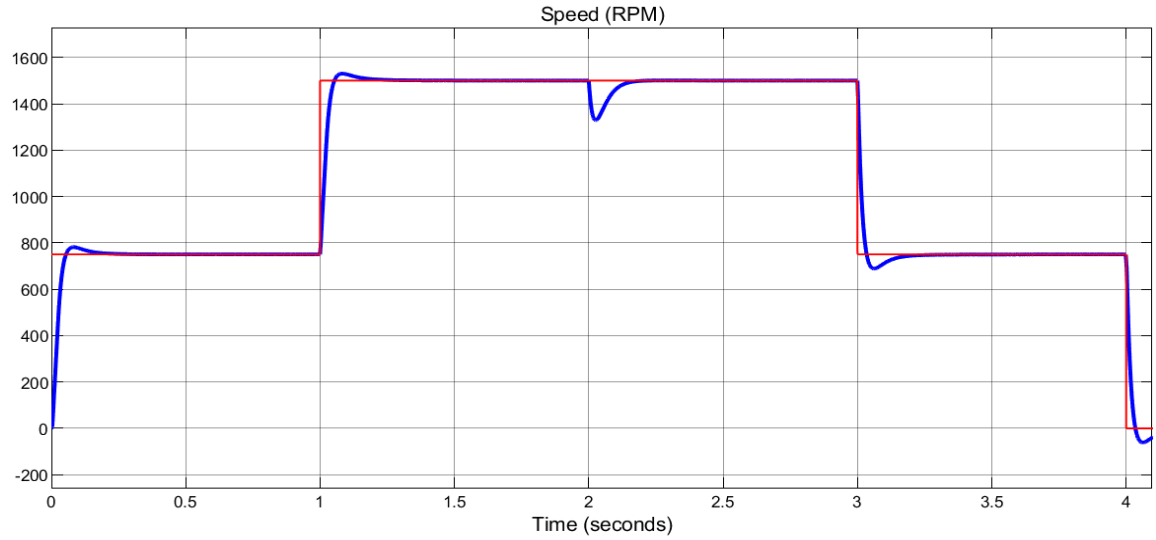

Fig. 8. Speed response

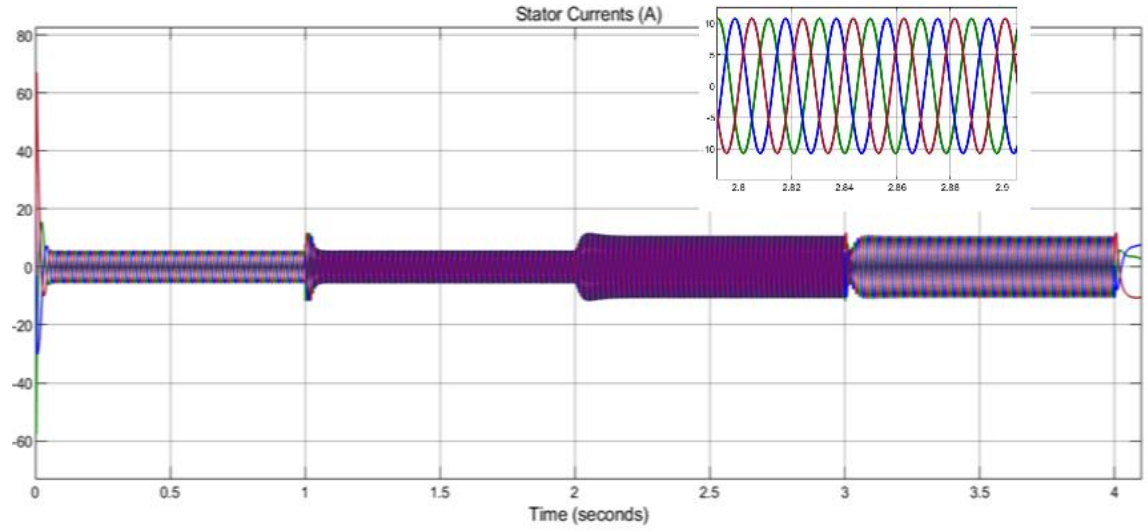

Fig. 9. Stator currents

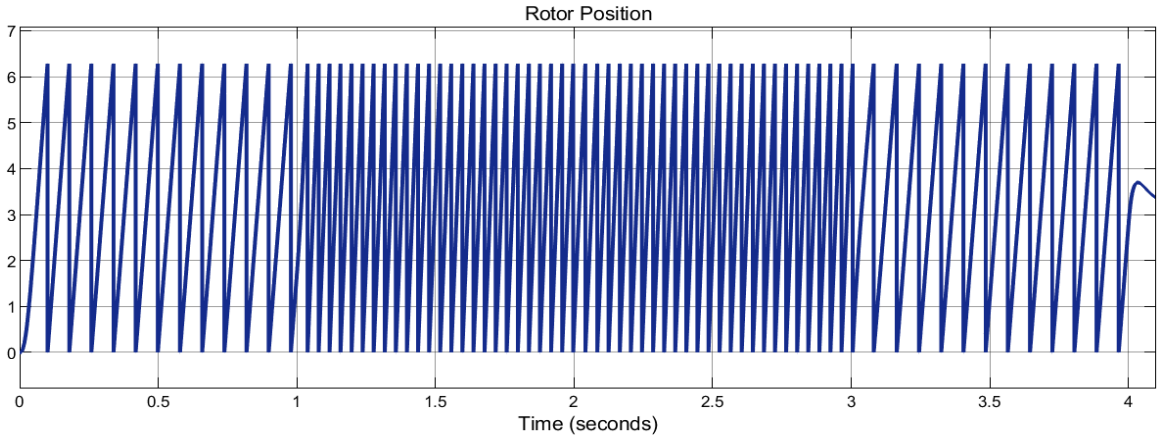

Fig. 10. Rotor angular position

Based on Table 4, it can be observed that circuit using SVPWM show lower THD compared to those using SPWM where the THD is decreased from 40.24% for SPWM method to 13.67% for the

SVPWM method. However, a SVPWM inverter requires more steps to compute the duty cycles and establish the optimal sequence of switching for performance.

6. Conclusion

This paper presents an improved method for controlling multilevel PWM inverters in three-phase IM systems using two Proportional-Integral (PI) controllers to enhance output quality and stability. To address the harmonics distortion problem, the paper investigated the impact of two five-level diode-clamped PWM inverters: Space Vector PWM (SVPWM) and Sinusoidal PWM (SPWM). Simulations in MATLAB/Simulink were used for analysis. The obtained results show that the optimized PI controllers based on SBA improves the motor performance for various operation conditions. Moreover, the comparison study shows that the five-level SVPWM scheme performs better in terms of reducing the threshold harmonic distortion (THD) of the output line voltage than the five-level SPWM inverter. These insights are valuable for motor control and power electronics. Future research possibilities include real-world applications and exploring a seven-level SPWM inverter.

Author Contribution: All authors contributed equally to the main contributor to this paper. All authors read and approved the final paper.

Funding: This research received no external funding.

Conflicts of Interest: The authors declare no conflict of interest.

References

[1] Z. Sabir, M. A. Z. Raja, D. Baleanu, R. Sadat and M.R. Ali, "Investigations of non-linear induction motor model using the Gudermannian neural networks," *Thermal Science*, vol. 26, no. 4B, pp. 3399-3412, 2022, https://doi.org/10.2298/TSCI210508261S.

[2] H. Al-Khazraji, R. M. Naji, and M. K. Khashan, "Optimization of sliding mode and back-stepping controllers for AMB systems using gorilla troops algorithm," *Journal Européen des Systèmes Automatisés*, vol. 57, no. 2, pp. 417-424, 2024, https://doi.org/10.18280/jesa.570211.

[3] A. Hamoudi and L. Rasheed, "Design of an adaptive integral sliding mode controller for position control of electronic throttle valve," *Journal Européen des Systèmes Automatisés*, vol. 57, no. 3, p. 729, 2024, https://doi.org/10.18280/jesa.570310.

[4] Z. N. Mahmood, H. Al-Khazraji, and S. M. Mahdi, "Adaptive control and enhanced algorithm for efficient drilling in composite materials," *Journal Européen des Systèmes Automatisés*, vol. 56, no. 3, pp. 507-512, 2023, https://doi.org/10.18280/jesa.560319.

[5] R. A. Kadhim, M. Q. Kadhim, H. Al-Khazraji, and A. J. Humaidi, "Bee algorithm based control design for two-links robot arm systems," *IIUM Engineering Journal*, vol. 25, no. 2, pp. 367-380, 2024, https://doi.org/10.31436/iiumej.v25i2.3188.

[6] H. Al-Khazraji, K. Al-Badri, R. Al-Majeez, and A. J. Humaidi, "Synergetic control design based sparrow search optimization for tracking control of driven-pendulum system," *Journal of Robotics and Control (JRC)*, vol. 5, no. 5, pp. 1549-1556, 2024, https://doi.org/10.18196/jrc.v5i5.22893.

[7] H. Al-Khazraji, C. Cole, and W. Guo, "Dynamics analysis of a production-inventory control system with two pipelines feedback," *Kybernetes*, vol. 46, no. 10, pp. 1632-1653, 2017, https://doi.org/10.1108/K-04-2017-0122.

[8] H. Al-Khazraji, "Optimal Design of a Proportional-Derivative State Feedback Controller Based on Meta-Heuristic Optimization for a Quarter Car Suspension System," *Mathematical Modelling of Engineering Problems*, vol. 9, no. 2, pp. 437-442, 2022, https://doi.org/10.18280/mmep.090219.

[9] G.W. Abedulabbas and F.R. Yaseen, “Sensorless Speed Control of a Brushless DC Motor Using Particle Filter (PF),” *Mathematical Modeling of Engineering Problems*, vol. 9, no. 6, pp. 1523-1531, 2022, https://doi.org/10.18280/mmep.090612.

[10] M.A. Hannan, J.A, Ali, A. Mohamed and A. Hussain, "Optimization techniques to enhance the performance of induction motor drives: A review," *Renewable and Sustainable Energy Reviews*, vol. 81, pp. 1611-1626, 2018, https://doi.org/10.1016/j.rser.2017.05.240.

[11] S. Rafa, A. Larabi, L. Barazane, M. Manceur, N. Essounbouli and A. Hamzaoui, "Implementation of a new fuzzy vector control of induction motor," *ISA transactions*, vol. 53, no. 3, pp. 744-754, 2014, https://doi.org/10.1016/j.isatra.2014.02.005.

[12] A. S. Kale, A. V. Tamhane and A. A. Kalage, "Comparative study of SPWM And SVPWM cascaded h-bridge multilevel inverter," *2017 International Conference on Intelligent Computing and Control (I2C2)*, pp. 1-6, 2017, https://doi.org/10.1109/I2C2.2017.8321785.

[13] Q. M. Attique, Y. Li and K. Wang, "A survey on space-vector pulse width modulation for multilevel inverters," *CPSS Transactions on Power Electronics and Applications*, vol. 2, no. 3, pp. 226-236, 2017, https://doi.org/10.24295/CPSSTPEA.2017.00021.

[14] N. Prabaharan and K. Palanisamy, "A comprehensive review on reduced switch multilevel inverter topologies, modulation techniques and applications," *Renewable and Sustainable Energy Reviews*, vol. 76, pp. 1248-1282, 2017, https://doi.org/10.1016/j.rser.2017.03.121.

[15] N. Karnik, D. Singla and P. R. Sharma, "Comparative analysis of harmonic reduction in multilevel inverter," *2012 IEEE Fifth Power India Conference*, pp. 1-5, 2012, https://doi.org/10.1109/PowerI.2012.6479521.

[16] T.F. Chan and K. Shi, “Applied intelligent control of induction motor drives,” *John Wiley & Sons*, 2011, https://doi.org/10.1002/9780470825587.

[17] Z. B. Ibrahim, M. L. Hossain, M. H. N. Talib, R. Mustafa and N. M. N. Mahadi, "A five level cascaded H-bridge inverter based on space vector pulse width modulation technique," *2014 IEEE Conference on Energy Conversion (CENCON)*, pp. 293-297, 2014, https://doi.org/10.1109/CENCON.2014.6967518.

[18] W. Zhang and Y. Yu, "Comparison of three SVPWM strategies," *Journal of Electronic Science and Technology*, vol. 5, no. 3, pp. 283-287, 2007, https://www.journal.uestc.edu.cn/en/article/pdf/preview/1964.pdf.

[19] Z. N. Mahmood, H. Al-Khazraji, and S. M. Mahdi, "PID-based enhanced flower pollination algorithm controller for drilling process in a composite material," *Annales de Chimie. Science des Materiaux*, vol. 47, no. 2, pp. 91-96, 2023, https://doi.org/10.18280/acsm.470205.

[20] M. A. AL-Ali, O. F. Lutfy, and H. Al-Khazraji, "Investigation of Optimal Controllers on Dynamics Performance of Nonlinear Active Suspension Systems with Actuator Saturation," *Journal of Robotics and Control (JRC)*, vol. 5, no. 4, pp. 1041-049, 2024, https://doi.org/10.18196/jrc.v5i4.22139.

[21] R. M. Naji, H. Dulaimi, and H. Al-Khazraji, "An optimized PID controller using enhanced bat algorithm in drilling processes," *Journal Européen des Systèmes Automatisés*, vol. 57, no. 3, pp. 767-772, 2024, https://doi.org/10.18280/jesa.570314.

[22] F. R. Yaseen, M. Q. Kadhim, H. Al-Khazraji, and A. J. Humaidi, "Decentralized control design for heating system in multi-zone buildings based on whale optimization algorithm," *Journal Européen des Systèmes Automatisés*, vol. 57, no. 4, pp. 981-989, 2024, https://doi.org/10.18280/jesa.570406.

[23] H. Al-Khazraji, K. Al-Badri, R. Almajeez, and A. J. Humaidi, "Synergetic control-based sea lion optimization approach for position tracking control of ball and beam system," *International Journal of Robotics and Control Systems*, vol. 4, no. 4, pp. 1547-1560, 2024, https://doi.org/10.31763/ijrcs.v4i4.1551.

[24] M. Q. Kadhim, F. R. Yaseen, H. Al-Khazraji, and A. J. Humaidi, "Application of Terminal Synergetic Control Based Water Strider Optimizer for Magnetic Bearing Systems," *Journal of Robotics and Control (JRC)*, vol. 5, no. 6, pp. 1973-1979, 2024, https://doi.org/10.18196/jrc.v5i6.23867.

[25] A. K. Ahmed, H. Al-Khazraji, and S. M. Raafat, "Optimized PI-PD control for varying time delay systems based on modified Smith predictor," *International Journal of Intelligent Engineering and Systems*, vol. 17, no. 1, pp. 331-342, 2024, https://doi.org/10.22266/ijies2024.0229.30.

[26] N. Alamsyah, A. L. Lubis, D. Hamdi, "Formulation of Marketing Strategies in Expedition Services Company with SWOT and QSPM Methods," *Proceedings of the International Manufacturing Engineering Conference & The Asia Pacific Conference on Manufacturing Systems*, pp. 3-9, 2019, https://doi.org/10.1007/978-981-15-0950-6_1.

[27] S. Khlil, H. Al-Khazraji, and Z. Alabacy, "Solving assembly production line balancing problem using greedy heuristic method," *IOP Conference Series: Materials Science and Engineering*, vol. 745, no. 1, pp. 1-7, 2020, https://doi.org/10.1088/1757-899X/745/1/012068.

[28] H. Al-Khazraji, "Comparative study of whale optimization algorithm and flower pollination algorithm to solve workers assignment problem," *International Journal of Production Management and Engineering*, vol. 10, no. 1, pp. 91-98, 2022, https://doi.org/10.4995/ijpme.2022.16736.

[29] G.W. Abedulabbas and F.R. Yaseen, "Design a PI controller based on PSO and GWO for a Brushless DC Motor," *Journal Européen des Systèmes Automatisés*, vol. 55, no. 3, pp. 331-333, 2022, https://doi.org/10.18280/jesa.550305.

[30] H. Al-Khazraji, W. Guo and A.J. Humaidi, "Improved cuckoo search optimization for production inventory control systems," *Serbian Journal of Electrical Engineering*, vol. 21, no. 2, pp. 187-200, 2024, https://doi.org/10.2298/SJEE2402187A.

[31] M. Ahmed and M. Msallam, "Enhancement performance of hydraulic actuators using PSO with FOPID controller," *Journal of Mechatronics and Artificial Intelligence in Engineering*, vol. 2, no. 1, pp. 19-29, 2021, https://doi.org/10.21595/jmai.2021.21872.

[32] M. Mohamed and L. Thamir, "Design of Nonlinear PID and FOPID Controllers for Electronic Throttle Valve Plate's Position," *Journal of Electrical and Computer Engineering*, vol. 2024, no. 1, p. 9984750, 2024, https://doi.org/10.1155/2024/9984750.

[33] P. D. Kusuma, and A. Dinimaharawati, "Swarm Bipolar Algorithm: A Metaheuristic Based on Polarization of Two Equal Size Sub Swarms," *International Journal of Intelligent Engineering & Systems*, vol. 17, no. 2, pp. 337-389, 2024, https://doi.org/10.22266/ijies2024.0430.31.

[34] F. R. AL-Ani, O. F. Lutfy, and H. Al-Khazraji, "Optimal Synergetic and Feedback Linearization Controllers Design for Magnetic Levitation Systems A Comparative Study," *Journal of Robotics and Control (JRC)*, vol. 6, no. 1, pp. 22-30, 2024, https://doi.org/10.18196/jrc.v6i1.24452.

[35] M. A. AL-Ali, O. F. Lutfy, and H. Al-Khazraji, "Comparative study of various controllers improved by swarm optimization for nonlinear active suspension systems with actuator saturation," *International Journal of Intelligent Engineering & Systems*, vol. 17, no. 4, pp. 870-881, 2024, https://doi.org/10.22266/ijies2024.0831.66.

[36] F. R. AL-Ani, O. F. Lutfy, and H. Al-Khazraji, "Optimal Backstepping and Feedback Linearization Controllers Design for Tracking Control of Magnetic Levitation System A Comparative Study," *Journal of Robotics and Control (JRC)*, vol. 5, no. 6, pp. 1888-1896, 2024, https://doi.org/10.18196/jrc.v5i6.24073.

[37] P. Jayal and G. Bhuvaneswari, "A novel space vector modulation-based transistor-clamped H bridge inverter-fed permanent magnet synchronous motor drive for electric vehicle applications," *International Transactions on Electrical Energy Systems*, vol. 31, no. 3, p. e12789, 2021, https://doi.org/10.1002/2050-7038.12789.

[38] T. A. Ahmed, E. E. M. Mohamed, A. Youssef and A. A. Ibrahim, "Review of Permanent Magnet Synchronous Motor Fed by Multilevel Inverter," *SVU-International Journal of Engineering Sciences and Applications*, vol. 1, no. 1, pp. 22-31, 2020, https://doi.org/10.21608/svusrc.2020.51244.1001.

[39] M. Rajkumar and P. Manoharan, "Modeling and simulation of five-level five-phase voltage source inverter for photovoltaic systems," *Journal Przeglad Elektrotechniczny*, vol. 10, no. 10, pp. 237-241, 2013, http://pe.org.pl/articles/2013/10/59.pdf.

[40] M. Khalid, A. Mohan and B. A. C, "Performance Analysis of Vector controlled PMSM Drive modulated with Sinusoidal PWM and Space Vector PWM," *2020 IEEE International Power and Renewable Energy Conference*, pp. 1-6, 2020, https://doi.org/10.1109/IPRECON49514.2020.9315210.

[41] S. K. Peddapelli, "Recent advances in pulse width modulation techniques and multilevel inverters," *International Journal of Electrical and Computer Engineering*, vol. 3, pp. 600-608, 2014, https://drive.google.com/file/d/1XX9wtaLZhIDHvJm3-LauvUxkoZj76sgc/view.

[42] G. Vivek, J. Biswas, A. K. Muthavarapu, M. D. Nair and M. Barai, "Optimised Design and Implementation of SVPWM Switching sequences for Five level VSI," *2018 IEEE International Conference on Power Electronics, Drives and Energy Systems (PEDES)*, pp. 1-6, 2018, https://doi.org/10.1109/PEDES.2018.8707569.

[43] S. Choudhury, S. Nayak, T. P. Dash and P. K. Rout, "A comparative analysis of five level diode clamped and cascaded H-bridge multilevel inverter for harmonics reduction," *2018 Technologies for Smart-City Energy Security and Power (ICSESP)*, pp. 1-6, 2018, https://doi.org/10.1109/ICSESP.2018.8376690.

[44] A. Hafeez *et al*., "Comparative Analysis of the PWM and SPWM on Three-Phase Inverter through Different Loads and Frequencies," *Journal of Computing & Biomedical Informatics*, vol. 4, no. 02, pp. 204-220, 2023, https://www.jcbi.org/index.php/Main/article/view/136.

[45] M. Murnane and I. Ono, "Simulink-Based SVPWM Current Control Technique for Multilevel Diode NPC Inverter Topologies," *Analog Devices*, 2013, https://www.analog.com/en/resources/technical-articles/simulink-based-svpwm-current-control-technique.html.

[46] A. Kumar, K. Gowri and M. Kumar, "New generalized SVPWM algorithm for multilevel inverters," *Journal of Power Electronics*, vol. 18, no. 4, pp. 1027-1036, 2018, https://doi.org/10.6113/JPE.2018.18.4.1027.

[47] Z. Liu, B. Li, X. Wang, X. Wu and F. Li, "A predictive control method for switching sequence selection based on SVPWM for five-level converter," *IET Power Electronics*, vol. 16, no. 6, pp. 990-1000, 2023, https://doi.org/10.1049/pel2.12445.

[48] R. Pawar, S. P. Gawande, S. G. Kadwane, M. A. Waghmare, R. N. Nagpure, "Five-level diode clamped multilevel inverter (DCMLI) based electric spring for smart grid applications," *Energy Procedia*, vol. 117, pp. 862-869, 2017, https://doi.org/10.1016/j.egypro.2017.05.204.

[49] G. Mademlis, "Medium voltage generation system with five-level NPC converters for kite tidal power,"*Master's thesis, Universidade Tecnica de Lisboa*, 2019, https://research.chalmers.se/en/publication/510092.

[50] H. Beleiu, S. Pavel, M. Birou, A. Miron, P. Darab and M. Sallah, "Effects of voltage unbalance and harmonics on drive systems with induction motor," *Journal of Taibah University for Science*, vol. 16, no. 1, pp. 381-391, 2022, https://doi.org/10.1080/16583655.2022.2064670.